

# WiCrew: Gait-based Crew Identification for Cruise Ships Using Commodity WiFi

Kezhong Liu, Dashuai Pei, Shengkai Zhang, Xuming Zeng, Kai Zheng, Chunshen Li, Mozi Chen

**Abstract**—Security check-in life-support areas, e.g., bridge, engine room, is crucial for cruise ships due to numerous and diverse passenger identities. Instead of conventional security check approaches, such as facial recognition and fingerprint identification, device-free approaches enabled by WiFi-based gait recognition have attracted considerable attention owing to their low cost, non-intrusiveness, and privacy protection. Despite the excellent performance of existing indoor methods, they cannot be trivially extended to cruise ships because of the unique characteristics of hull deformation caused by vibrating engines and waves. This stems from the flexible structure of cruise ships, which introduces additional noise to the WiFi signals. To address this challenge, we propose WiCrew, a device-free gait recognition system that detects crew identity anomalies in cruise ships. WiCrew consists of two components: 1) a spatial separation algorithm that separates the signal components from ship vibration and human activity; 2) a speed-independent adversarial learning framework that identifies the ship's crew using human gaits at an arbitrary walking speed. Extensive experiments on a cruise ship demonstrate the effectiveness of WiCrew. While the crew members walk at speed of 0.7 to 1.8 m/s, the average recognition accuracy reaches 82%, which is similar to vision-based approaches.

**Index Terms**—WiFi signals, Gait recognition, Cruise ship, device-free sensing.

## I. INTRODUCTION

SECURITY check is crucial in cruise ships due to their long journey with the complicated identities of tourists [1]. In particular, the bridge, engine room, and cargo hold of a ship are related to life support and property protection. Recent studies (e.g., [2] [3] [4]) have shown that fatal accidents may lack identity recognition systems in cruise ships. Thus, it is desirable to identify crew members in these sensitive areas during the day and night periods.

Internet of Things (IoT)-based identity authentication technologies have gained considerable attention in industry

Manuscript received XX XXX, 2022; revised XX XXX, 2022.

This work was supported by the National Natural Science Foundation of China (NSFC) under Grant No. 51979216, and the Natural Science Foundation of Hubei Province, China, under Grant No.2021CFA001.

Kezhong Liu is with the School of Navigation, National Engineering Research Center for Water Transport Safety, and Hubei Key Laboratory of Inland Shipping Technology, Wuhan University of Technology, Wuhan 430063, China (e-mail: kzliu@whut.edu.cn).

Mozi Chen, Dashuai Pei, Xuming Zeng and Kai Zheng are with the School of Navigation, Wuhan University of Technology, Wuhan 430063, China (e-mail: chenmz, 291623, zengxuming, kzhseng@whut.edu.cn).

Shengkai Zhang is with the School of Information Engineering, Wuhan University of Technology, Wuhan 430063, China (e-mail: shengkai@whut.edu.cn).

Chunshen Li is with the School of Electronic Information and Communications, Huazhong University of Science and Technology, Wuhan, 430074 China (e-mail: leechechsh@hust.edu.cn).

(Corresponding author: Mozi Chen)

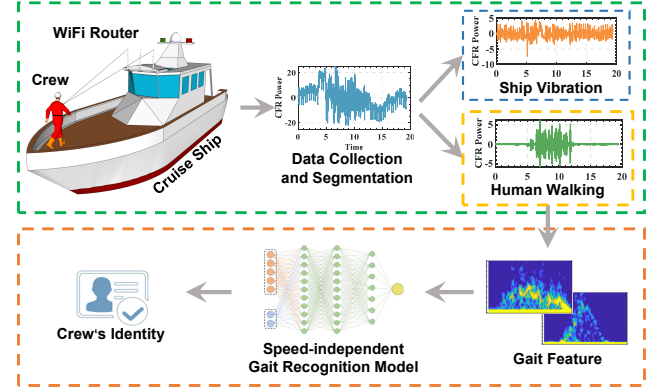


Fig. 1: Our proposed WiCrew uses commercial Off-The-Shelf (COTS) WiFi devices deployed on the cruise ship to implement gait-based crew identification.

and academia due to their low cost and ease of deployment [5] [6] [7]. They use biological information such as fingerprints, eyes, and facial features to authorize access to sensitive areas. Nevertheless, such biological information can either be intrusive or compromise privacy [8] [9]. Thus, researchers propose device-free sensing systems using radio frequency (RF) signals to provide non-intrusive and privacy-preserving identity authentication services [10]. Specifically, they take the pattern of gaits as fingerprints to identify humans.

RF-based gait recognition technology captures gait through radio frequency signals reflected by the human body, which can work effectively under non-line-of-sight (NLoS) conditions and is unaffected by light conditions. Typically, RF-based gait recognition using RFID [11] [12], mmWave radar [13] [14], and WiFi [15] [16] has gained considerable attention in academia. Among them, WiFi is the most promising candidate for cruise ships because the existing onboard WiFi APs are available for gait recognition.

Unfortunately, the existing WiFi-based gait recognition cannot be trivially extended to work on cruise ships. The unique environmental characteristic of ships is hull vibration [17] [18] [19], which severely distorts WiFi signals, making it much more difficult to extract human reflections. Therefore, the gait signals are distorted, resulting in inaccurate gait recognition results. In addition, current WiFi-based gait recognition [20] [21] assumes that the walking speed of the target is consistent in the training and testing stages. However, crews and passengers often change walking speed due to their health status, mood, load-bearing status, and other factors leading to a deviation between the source and target domains.

At the same time, most of the gait parameters, such as gait cycle and step length, are speed-dependent [22] [23], and the change in speed leads to changes in these parameters.

In this study, we propose **WiCrew**, which uses commercial COTS WiFi devices deployed on a cruise ship to capture fine-grained gait features so that we can recognize the crew's identity, as shown in Figure 1. Three key characteristics of the WiCrew make it a reliable solution for passive crew identification. First, WiCrew can automatically detect the walking behavior of the crew and implement a gait-based crew identification. Second, WiCrew can overcome the WiFi signal interference from the hull vibration by performing a spatial signal decomposition algorithm. Third, WiCrew is immune to changes in the crew's walking speed by extracting speed-independent gait features.

To realize WiCrew, we overcome two critical challenges. First, the direct use of channel frequency response (CFR), collected in the ship room, in gait recognition is challenging because hull vibration severely distorts the WiFi signals. Second, most of the gait parameters, such as step size, gait cycle time, and stride frequency, are speed-dependent, which results in the low robustness of existing gait-based identification techniques when the target speed changes.

To tackle the challenges mentioned above, we first propose a frequency band energy threshold-based walking activity determination and segmentation method to automatically determine whether a crew member is walking in the background and extract signal segments containing walking activity. Second, we model the separation hull vibration and crew's walking activity as blind source separation (BSS) problems and propose a vibration-activity separation algorithm based on empirical mode decomposition [24] and independent component analysis [25] (EMD-ICA). Third, we propose a speed-independent and identity-discriminable gait feature extraction method based on a domain adversarial neural network and use these features for identity recognition.

In summary, we make the following contributions.

- We propose a crew walking activity detection method, which can automatically detect crew's walking behavior and extract signal fragments containing walking activity.
- We propose a vibration-activity separation algorithm that can separate hull vibrations from crew walking activities.
- To extract speed-independent gait features, we propose a gait recognition model based on a domain adversarial neural network (DANN).

The remainder of this paper is organized as follows. Related studies on traditional gait recognition and WiFi-based gait recognition are reviewed in section 2. In section 3 introduces preliminary observations. Section 4 introduces the system overview and the system design about vibration-activity separation and speed-independent gait recognition model in sections 5 and 6. Section 7 describes the experimental setup and evaluation. Finally, we conclude the paper in section 8.

## II. RELATED WORK

Our work focuses on identifying people by detecting gait patterns, which is divided into traditional gait recognition and WiFi-based gait recognition.

### A. Traditional Gait Recognition

There are three basic types of sensors used in conventional gait identification technology: cameras, wearable sensors (such as pedometers), and floor sensors. At present, camera-based gait recognition technology achieves high recognition accuracy. Lee et al [26] proposed a gait recognition model based on ellipse parameters, which divides the human body into seven ellipses, and calculates the parameter changes of the seven ellipses during the human movement process to construct a gait representation. Another classic solution is to crop the silhouettes of persons in the video frame by frame and then stack them up to generate a gait energy map (GEI) [27]. Nonetheless, this method requires enough lighting and line-of-sight (LoS) path. Moreover, they often cause privacy issues among users [28] [29] [30]. WiCrew, on the other hand, is independent of illumination conditions and can function in dark areas. Moreover, they do not capture target images and can protect privacy more effectively. Wearable sensor-based gait recognition techniques require the target to wear sensors such as IMU and gyroscopes all the time to extract acceleration or rotation variance during walking. However, this method requires users to wear it for a long time, which may cause discomfort [31] [32] [33]. The WiCrew system is a device-free passive gait recognition system that does not require the user to wear a device. Floor sensor-based gait recognition technology utilizes sensors installed under the floor, such as pressure sensors, to capture gait characteristics, such as plantar pressure distribution [34]. However, this approach is complex to deploy and is implemented only in specialized areas. By leveraging existing WiFi APs, the WiCrew solution reduces installation costs and complexity.

### B. WiFi-based Gait Recognition

In recent years, WiFi-based gait recognition technology has attracted considerable attention in intelligent furniture, intrusion detection, and other fields. WiWho [20] system extracts CSI signals in the 0.3-2 Hz band, which analyzes gait parameters such as the gait cycle and the number of steps. WiFiU [21] uses principal component analysis and spectral subtraction to obtain high-quality spectrograms from which gait cycles and more than 170 other features can be extracted to identify people. WiFi-ID [35] extracts features within the 20-80 Hz frequency band and uses a sparse approximate classifier to identify identities. AGait [36] considered that previous work required subjects to have fixed walking path and direction and tried to use two WiFi links to obtain gait features independent of path and direction, and used them to identify people. GaitSense [37] extracted the gait pattern from six WiFi links and eliminated irrelevant disturbances using a normalization algorithm. GaitFi [38] proposes an innovative multimodal gait recognition method that uses WiFi signals and videos for human identification. MetaGanFi [39] proposes a domain-agnostic meta learning model, DA-Meta that could quickly adapt from one/few data samples to accurately recognize unseen individuals. However, the aforementioned static environment-based solutions degrade dramatically when deployed directly on a ship due to the ship's unique environ-

ment. Our solution was built specifically for a dynamic ship environment and is able to effectively reduce noise from ship vibrations.

### III. PRELIMINARY AND OBSERVATION

In this section, we first provide preliminary knowledge about the CFR power model. Next, we present three observations: walking activity affects CFR, hull vibration affects CFR, and walking speed affects gait shape description.

#### A. CFR Power Model

The CFR power model describes the influence of human motion on a WiFi signal in a static environment [21]. WiFi signal from the sender can directly travel through the line-of-sight (LoS) path or be reflected off the wall and the walking human, and propagate through multiple paths before arriving at the receiver. This phenomenon is known as the multipath effect. If a WiFi signal arrives at the receiver through  $N$  different paths, then  $H(f, t)$  is given by the following equation:

$$H(f, t) = e^{-j2\pi\Delta ft} \sum_{k=1}^N a_k(f, t) e^{-j2\pi f\tau_k(t)}, \quad (1)$$

where  $a_k(f, t)$  is the complex-valued representation of the attenuation and initial phase offset of the  $k^{th}$  path,  $e^{-j2\pi f\tau_k(t)}$  is the phase shift on the  $k^{th}$  path with a propagation delay of  $\tau_k(t)$ , and  $e^{-j2\pi\Delta ft}$  is the phase shift caused by the carrier frequency difference  $\Delta f$  between the sender and the receiver.

The CFR power model divides multipaths into static (reflected on stationary objects and LoS paths) and dynamic paths (reflected from walking targets). The dynamic path changes as users move and is the sum of the CFRs of all those paths that arrive at the receiver after reflecting from the moving body parts of the users. The static path is not affected by the movement of any user and is the sum of the CFRs of all those paths that arrive at the receiver without reflecting from any moving body parts. If there exist  $N_d$  dynamic and static paths are denoted by  $H_s(f)$ , the CFR  $H(f, t)$  can be roughly expressed as

$$H(f, t) = e^{-j2\pi\Delta ft} \left( H_s(f) + \sum_{k \in N_d} a_k(f, t) e^{-j\frac{2\pi d_k(t)}{\lambda}} \right), \quad (2)$$

Let  $v_k$  represent the rate at which the length of the  $k^{th}$  path changes. The length  $d_k(t)$  of the  $k^{th}$  dynamic path at time  $t$  is expressed as  $d_k(t) = d_k(0) + v_k t$ . The instantaneous CFR power at time  $t$  can be derived as follows

$$\begin{aligned} |H(f, t)|^2 &= \sum_{k \in N_d} 2 |H_s(f) a_k(f, t)| \cos \left( \frac{2\pi v_k t}{\lambda} + \frac{2\pi d_k(0)}{\lambda} + \phi_{sk} \right) \\ &+ \sum_{k, l \in N_d} 2 |a_k(f, t) a_l(f, t)| \cos \left( \frac{2\pi (v_k - v_l) t}{\lambda} + \frac{2\pi (d_k(0) - d_l(0))}{\lambda} + \phi_{kl} \right) \\ &+ \sum_{k \in N_d} |a_k(f, t)|^2 + |H_s(f)|^2, \end{aligned} \quad (3)$$

where  $\frac{2\pi d_k(0)}{\lambda} + \phi_{sk}$  and  $\frac{2\pi (d_k(0) - d_l(0))}{\lambda} + \phi_{kl}$  are constants that represent the initial phase offsets for the different paths.

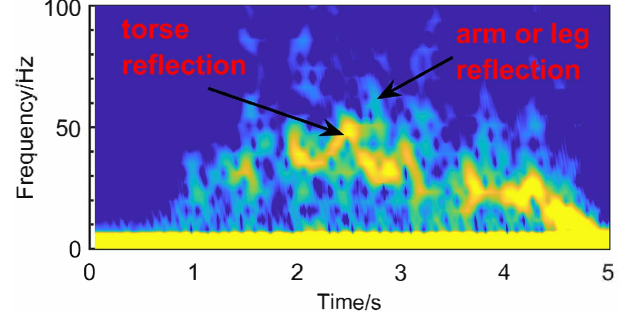


Fig. 2: The CFR power spectrogram of human walking.

Eq.(3) indicates that the total CFR power is the sum of a constant offset and a set of sinusoids, where the frequencies of the sinusoids are functions of the rate of path length changes. Next, we present three valuable insights from Eq.(3), and describe how this useful information guide the design of removing the ship vibration of WiCrew.

#### B. Experiments and Observations

In this section, we describe some experiments and observations that illustrate the practical challenges encountered when implementing WiCrew.

##### 1) Observations 1: Different individuals' gaits produce unique patterns in the aggregate CFR power.

According to the CFR power model, when a stationary target starts walking, the movement of the target introduces new frequency components into the CFR power. Similarly, a few CFR power frequency components disappear when the target stops walking, as shown in Figure 2. This phenomenon indicates that the start and end of user's walking behavior can be determined by the energy of the corresponding frequency component in the CFR power. Specifically, when a person begins and stops walking, the energy in the frequency band of 30-50 Hz of the CFR power is always changed. The reason for not choosing the 0-30 Hz range is that the CFR power change due to human in-place activities tends to be below 30 Hz.

However, during human walking, the speed of each part of the body is different (e.g., the hand moves faster than the trunk), so the path change speed of the WiFi signal reflected by each part is different. As shown in Figure 2, we observed a high energy ("hot" colored) band, which corresponds to torso reflection. There are several low-energy bands around the torso reflection, which is an arm or leg reflection. This shows that because different people's gaits involve movements of body parts at different speeds, each individual's gait produces a unique pattern in the aggregate CFR power. By learning this unique pattern, the WiCrew system can achieve a gait recognition task.

##### 2) Observations 2: Ship vibrations while sailing can severely distort WiFi signals.

Due to external stresses such as loads, waves, and engines, a ship vibrates continuously when sailing. The CFR power value of a ship's indoor environment has characteristics distinct from those of land due to ship vibration. At various phases of sailing, the hull vibrates at varying intensities. For instance,

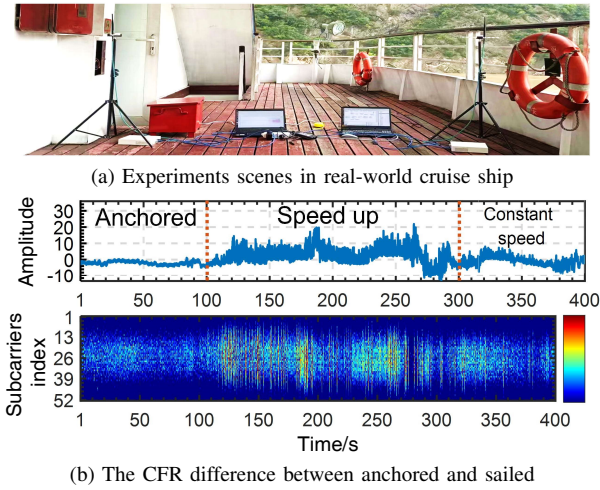


Fig. 3: CFR profiles of real-world cruise ships in three different phases.

when a ship is anchored, the hull vibrates with a tiny amplitude due to wave action. When the ship cruises at a constant speed, the hull is subjected to the combined action of waves, loads, and engines, and the vibrations are noticeable. As when the ship accelerates, hull vibrations increase.

In order to further illustrate the influence of hull vibration on the CFR value, we conducted experiments in the real-world ship environment, and the study setup is shown in Figure 3(a). We collected CFR signals in the ship environment in three phases: anchoring, speed up, and constant speed, ensuring no interference from other factors during the entire experiment. It can be seen in Figure 3(b) that the CFR value remains constant while the ship is anchored. Gait recognition using WiFi is now quite accurate. The ship then began accelerating away from the dock, at which point the CFR power fluctuated wildly with the motion of the ship. This demonstrates that the hull's vibrations vary depending on the sailing phase. At a certain point, the ship stabilized at a constant speed, and the CFR power variations decreased and stabilized.

### 3) Observations 3: Gait shape description can be significantly affected by the change of walking speed.

Most gait-based identification systems can be very reliable if the user walks at the same speed all the time. However, the variation of walking speed will significantly affect the description of gait shape. For example, if you walk slowly, your stride length and gait cycle may get shorter. Also, the difference in walking speed between the training set and the test set makes the source domain and the target domain different. Because of this, a gait recognition model that was trained for a certain walking speed is usually not good at predicting gait samples at any walking speed.

We used real-world experimental data to show that different walking speeds result in distinct gait shape descriptions. First, we fixed the smartbands on the person's ankle and collected the X-axis acceleration sensor data when the person was walking. The experimental setup is illustrated in Figure 4(a). Next, we show the gait shape descriptions of different people within the same walking speed range in Figure 4(b). It can

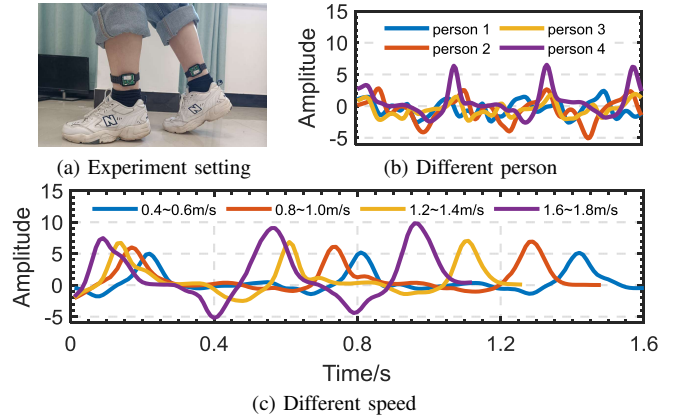


Fig. 4: Walking speed affects gait shape description

be seen that the gait shape descriptions of different people are very different, which indicates that gait information can be used to distinguish a person's identity. Finally, we show the gait shape description of the same person at different walking speed ranges, as shown in Figure 4(c). Apparently, the gait shape description changes with the speed change but still maintains a considerable similarity, which indicates that the speed can significantly affect the gait shape. However, the speed-independent gait features still do not change with speed.

## IV. SYSTEM OVERVIEW

Our research aims to implement a speed-independent gait recognition system for the dynamic environment of a ship. WiCrew consists of three main components: data collection and preprocessing, vibration-activity separation technology, and a DANN-based speed-independent gait recognition model, as shown in Figure 5.

- Data Collection and Pre-processing.** WiCrew collects CSI measurements on the receiving end of a WiFi link between two WiFi devices, and calculates CFR power. To reduce data redundancy and irrelevant noise between subcarriers, principal component analysis (PCA) is used to pre-process CFR power.
- Vibration-activity Separation.** To automatically detect and segment walking activity in CFR power, we proposed a walking activity determination and segmentation method based on frequency band threshold. We introduced a vibration-activity separation algorithm based on the captured walking activity signal fragments to remove the ship vibration components.
- Speed-independent Gait Recognition Model.** Finally, to extract speed-independent and identity-discriminable gait features and realize gait-based crew identification, we first normalized the input data with data format converter, and then completed crew identity recognition with speed-independent gait recognition model based on DANN.

## V. VIBRATION-ACTIVITY SEPARATION

This section describes the separation of human walking activity from hull vibrations. First, we preprocessed the collected CFR signals. Second, the signal fragments containing

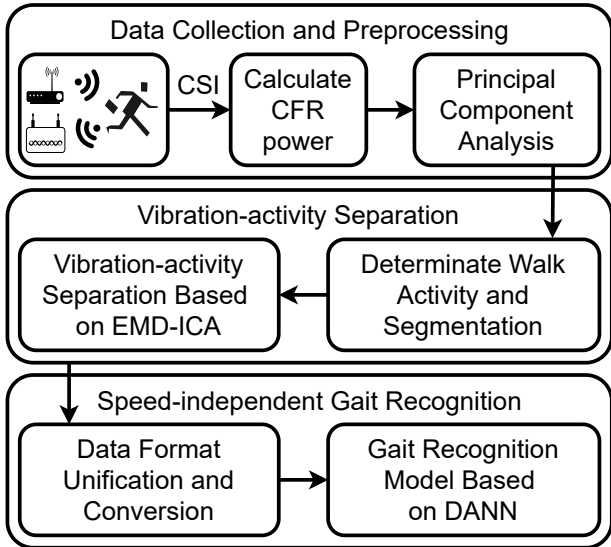


Fig. 5: System overview.

the walking activity were extracted. Finally, we proposed a vibration-activity separation algorithm to complete the vibration activity separation process.

#### A. CSI Collection and Pre-processing

In this section, we first collect CSI measurements from WiFi signals using commercial WiFi devices. Using the CSI tool, we collected CSI measurements from 30 OFDM subcarriers between each transmitting and receiving antenna pair. Thus, we obtained  $1 \times 3 \times 30 = 90$  CSI values for each received 802.11n frame when the sender has one antenna, and the receiver has three antennas. Because our system sends 1,000 WiFi frames per second, we collected 1,000 CSI values for each of the 90 CSI streams in one second. Each subcarrier CSI value of a sequence for a given transmit/receive antenna is called a CSI stream.

Next, we considered the raw CSI stream as the input and convert each CFR value in each stream to CFR power by multiplying it by its complex conjugate. Furthermore, we removed the constant offset caused by the static reflection path from the CFR power stream. A constant offset can be obtained by calculating the background CFR power in a long-term static environment. We used the PCA method to extract the first principal component from correlated CSI measurements to reduce irrelevant noise in different subcarriers [40]. Specifically, we cut the CFR power stream with a constant offset removed into chunks, and the size of each chunk had a sampling interval of 1-s. The PCA algorithm was applied to each chunk to obtain the principal components of the stream. The reason for choosing one 1-s as the block length is that the number of samples was large enough to ensure accurate correlation estimation, and the short time interval ensures the real-time performance of the system. For ease of writing and understanding, we refer to the processed data stream as *CSI power stream*.

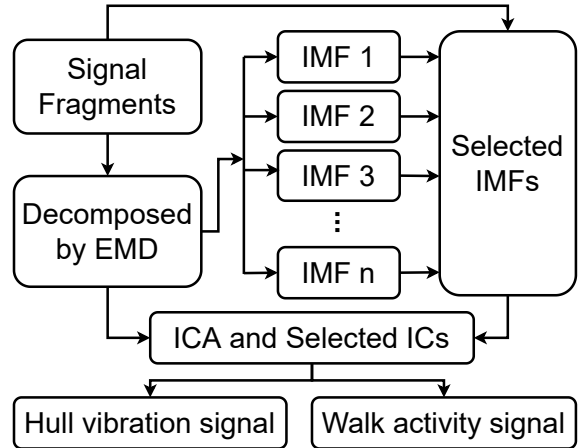


Fig. 6: Vibration-activity separation algorithm based on EMD-ICA.

#### B. Walking Determination and Segmentation

Before separating human walking activities from the vibrating ambient noise, WiCrew first determines whether people walk in an environment of interest and extracts signal fragments containing walking activity. However, ship vibrations cause CSI fluctuations, which will overwhelm the movement of people far away from the WiFi link. This means that traditional methods for figuring out walking activity based on variance won't work. So, we propose a method for figuring out and separating walking activities that is strong enough for ship sailing scenarios.

We propose a frequency-band energy-threshold walking-activity detection technology. Specifically, we detected signal energy of *CSI power stream* in the frequency range of 30~50 Hz as the basis for determining walking activities. This is because, when a person's walking speed is between 0.8 and 1.5 m/s, the fluctuation of the CFR power frequency under the 5180 MHz WiFi channel (carrier wavelength = 0.0579 meters) is between 30 and 50 Hz. When the detected energy was greater than the threshold, the walking activity starts, and the walking activity ends when the energy drops below the threshold. Detailed steps are presented in Algorithm1.

#### C. Vibration-activity Separation Algorithm

This section shows that separating the hull vibration signal from the walking activity signal can be modeled as a blind source separation (BSS) problem. Because we only used a pair of WiFi devices to measure the CSI, our problem is known as the single-channel blind Source separation problem (SCBSS). To solve the SCBSS problem, empirical mode decomposition (EMD) decomposes the signal and constructs multiple virtual observation channels. We can then use independent component analysis (ICA) to solve the BSS problem and remove hull vibration noise. The vibration-activity separation algorithm is shown in Figure 6.

**ICA requirements.** Assuming that all the sources are independent, non-Gaussian, and linearly combined, the BSS problem can be solved using ICA. To test this hypothesis,

**Algorithm 1** Frequency-band Energy Based Walking Activity Determination and Segmentation.

**Input:**

 Read input current signals  $x_{cur}$ ;

**Output:**

 Signal fragments containing walking activity  $x_{walk}$ ;

- 1: Defined operating parameters such as window size ( $n$ ), window type ( $w[n]$ ), hopping size ( $H$ ), sampling rate ( $f_s$ ), threshold ( $T$ )
- 2: Define variables and initialize them such as frame time ( $t_f = 0$ ), frame energy ( $E[t_f] = 0$ ),  $i = 0$ ,  $Duration[i] = 0$ ,  $Start = 0$ ,  $End = 0$ ;
- 3: Input signal  $x_{cur}$  is filtered by Butterworth bandpass filter with passband frequency of 30~50Hz;
- 4: **while**  $(n + H) \leq$  total of Input signal  $x_{sig}$  **do**
- 5:    $x \leftarrow x_{cur}[1 : n]. * w[n];$
- 6:    $frametime \leftarrow frametime + n/f_s;$
- 7:    $E[t_f] \leftarrow E[t_f] + x.*x;$
- 8:   **if**  $E[t_f] \geq T$  **then**
- 9:      $Duration[i] = t_f;$
- 10:   **end**
- 11:   **if**  $E[t_f] \leq T$  **then**
- 12:      $Start = Duration[0] \times n/f_s;$
- 13:      $End = Duration[-1] \times n/f_s;$
- 14:   **end**
- 15:   **if**  $End - Start \leq 5$  **then**
- 16:      $End = 0, Start = 0;$
- 17:   **else**
- 18:      $x_{walk} \leftarrow x_{cur}[Start : End];$
- 19:   **end**
- 20:    $x \leftarrow x_{cur}[1 + H : n + H];$
- 21:    $i = i + 1;$
- 22:   Go back step 4
- 23: **end while**

we first examined the independence of possible sources (hull vibration and human walking activity). Similarly, experiments were conducted in a real-world ship environment. We collected CSI signals of human walking activities in the ship anchoring state and CSI signals of the no-person environment in the ship sailing state. Next, we calculated the correlation between the CSI signals of the two groups. Figure 7 shows the correlation between walking activity and hull vibration, and it is evident that the correlation is less than 0.3. Thus, we conclude that human activity and hull vibrations are independent. To demonstrate the non-Gaussian nature of the source, we show the CSI power distributions for hull vibration and walking activity, in Figure 8. We can observe that these distributions are nonGaussian. We have demonstrated this earlier using the CSI power model to determine whether the combination of sources is linear. Therefore, ICA can be applied to CSI power data to separate hull vibration and walking activity.

**The Separation Model.** The SCBSS is an extremely under-determined condition of blind source separation (BSS), which can describe an observation signal instantaneously mixed by several unknown source signals passing through an anonymous

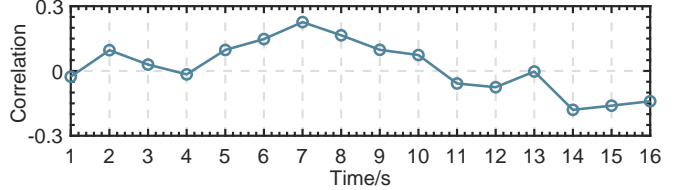


Fig. 7: Correlation between hull vibration and human walk activity.

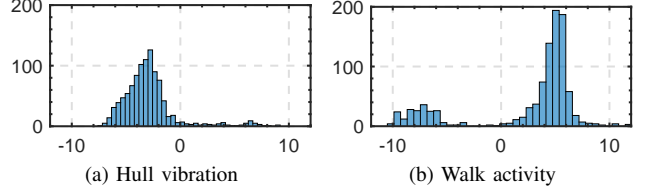


Fig. 8: Illustration of non-gaussian distributions of the hull vibration and human walk activity.

channel transmission matrix.

$$y(t) = \sum_{i=1}^N Cx_i(t), \quad (4)$$

where  $x_i(t) = [x_1(t), x_2(t), \dots, x_M(t)]^T$  denotes the unknown source signal,  $y(t)$  denotes the observed mixed signal,  $C$  denotes the unknown channel matrix, and  $N$  denotes the number of source signals.

The traditional blind source separation (BSS) problem is solved by ICA, which needs the number of observed signal channels to be greater than the number of source signals. This means that ICA can't directly solve the SCBSS problem. One way to solve the problem of SCBSS is to decompose the observation signal appropriately to construct multiple virtual observation channels and then extract the independent principal components through ICA. Because the CSI signal is a typical nonstationary signal, EMD decomposes the observed signal and constructs multiple observation channels. Here are the steps in more detail.

1) *Signal Decomposition Based on EMD:* In this section, we first decompose the signal to build a virtual observation channel. Based on the basic assumption that any signal is composed of several IMFs, EMD can decompose the original signal into high- and low-frequency IMFs. Thus, the original signal  $x(t)$  can be written as:

$$x(t) = \sum_{i=1}^n c_i(t) + r_n(t), \quad (5)$$

where  $c_i(t)$  represents the IMF and  $r_n(t)$  represents the residual component.

2) *IMFs Selection Based on Correlation:* Among the IMF obtained through EMD, low-frequency IMFs are producing to false modal components. High-frequency IMFs are prone to noise-dominated modal components, which can harm subsequent feature extraction. Therefore, adopting effective methods to screen for extracted IMF is necessary. This study adopted a correlation coefficient to measure the similarity between the IMF and the original signal. An IMF with low similarity is

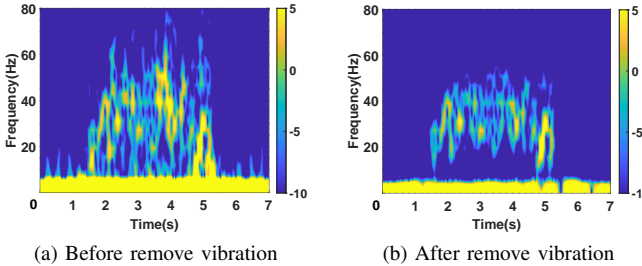


Fig. 9: The comparison between before and after removal of hull vibration

discarded by empirically setting the threshold. The correlation coefficients of  $x(n)$  and  $y(n)$  sequences are calculated using the following formula.

$$\rho_{xy} = \frac{\sum_{n=0}^{\infty} x(n)y(n)}{\sqrt{\sum_{n=0}^{\infty} x^2(n) \sum_{n=0}^{\infty} y^2(n)}}, \quad (6)$$

3) *Independent Components Analysis by FastICA*: The purpose of ICA is to decompose mixed signals into independent subcomponents. The solving model of ICA is

$$\hat{S} = W y(t) = W C x(t), \quad (7)$$

where  $\hat{S}$  is an estimate of  $x(t)$ ,  $W = \hat{C}^{-1}$  is the decomposition matrix, and  $\hat{C}$  is an approximation of the inverse of the channel-mixture matrix  $C$ . FastICA is an improved ICA algorithm with a faster convergence speed and no step-size parameter. This study used the FastICA algorithm to extract independent principal components from multiple IMFs.

Finally, using the vibration-activity separation algorithm based on EMD-ICA, we removed the hull vibration from the CFR power, as shown in Figure 9. Evidently, after using the vibration-activity separation algorithm, the hull vibration component is removed and the walking activity component is retained.

## VI. SPEED-INDEPENDENT GAIT RECOGNITION BASED ON DOMAIN ADVERSARIAL NEURAL NETWORK

The proposed speed-independent gait recognition model based on domain adversarial training comprises four parts: *data format converter*, *feature extractor*, *identity recognizer*, and *domain discriminator*. An overview of the model is shown in Figure 10. As mentioned above, the goal of the proposed model is to capture a speed-independent and identity-discriminative feature representation from a signal fragment containing a walking activity.

To achieve this goal, we first designed a **data format converter** to convert one-dimensional data of different lengths into two-dimensional matrices of the same size as the input data format to improve the feature expression ability. Then, the **feature extractor** based on CNN converts the input image into a latent representation, maximizes the accuracy of identity prediction using the **identity recognizer**, and obtains the predicted identity. The **domain discriminator** is used to maximize the recognition accuracy of the domain (*specifically, to identify the walking speed of the target as it walks*); however,

our design goal is to learn domain-independent features, which seems to create a contradiction. Therefore, in our design, using the gradient reversal layer, the feature extractor attempts to deceive the domain discriminator and improve the prediction accuracy of the identifier. The feature extractor can learn speed-independent and identity-discriminative features using this minimax game. The details of our neural network model are discussed in this section.

### A. Data Format Convertor

Because of the different gait cycles of each person, the time required to walk on a specific path is different; therefore, the length of the extracted signal fragments containing walking activities is different. To unify the data format, we first need to unify all signal fragments to the same length. We define the gait signal fragments  $Z$  as

$$Z = [z(1), z(2), \dots, z(i), \dots, z(o)], Z \in \mathbb{R}^o. \quad (8)$$

Here,  $o$  is the length of each input  $Z$ . As the time durations of the walking activities are different, the lengths  $o$  for different inputs  $Z$  are different. To unify the data length, we chose the maximum size of all signal fragments as the reference:  $o_{length} = o_{longest}$ . We pad data shorter than  $o_{longest}$  with zeros at the end.

Furthermore, to facilitate the use of CNN to extract features, one-dimensional data must be converted into a two-dimensional matrix. Considering that the time-frequency diagram contains motion characteristics of each part of the human body, we use the short-time Fourier transform (STFT) to transform the signal into a two-dimensional time-frequency image to enhance the feature expression ability. By setting the window function  $g(x)$ , window length  $windows\_size$ , overlapping length  $overlap\_size$  of two adjacent windows, and length  $fft\_size$  of the FFT, we can convert the original signal  $Z$  into a time-frequency graph  $X_{m \times n}$  using the following formula:

$$X(m, n) = \sum_{k=-\infty}^{\infty} Z(k)g^*(kT - mT)e^{-j\pi(nF)k}, \quad (9)$$

$$m = \frac{\text{length}(Z(k)) - windows\_size}{windows\_size - overlap\_size}, \quad (10)$$

$$n = \frac{fft\_size}{\text{length}(Z(k))} + 1, \quad (11)$$

Compared with the original signal, the generated two-dimensional time-frequency graph has a relationship between each value and the adjacent value and contains more details of human movement.

We let the time-frequency image  $X_i(m, n)$  be the input data of the proposed model. Each labeled data  $X_i(m, n)$  has both identity label  $y_i \in \mathcal{Y}$  and domain label  $d_i \in \mathcal{D}$ , where  $\mathcal{Y}$  and  $\mathcal{D}$  are the identity set and walking speed set of all subjects. We call labeled data the source domain and unlabeled data the target domain. Therefore, in the training phase, the input of our model is a 2D time-frequency graph  $X(m, n)$ , identity label  $y$ , and domain label  $d$ .

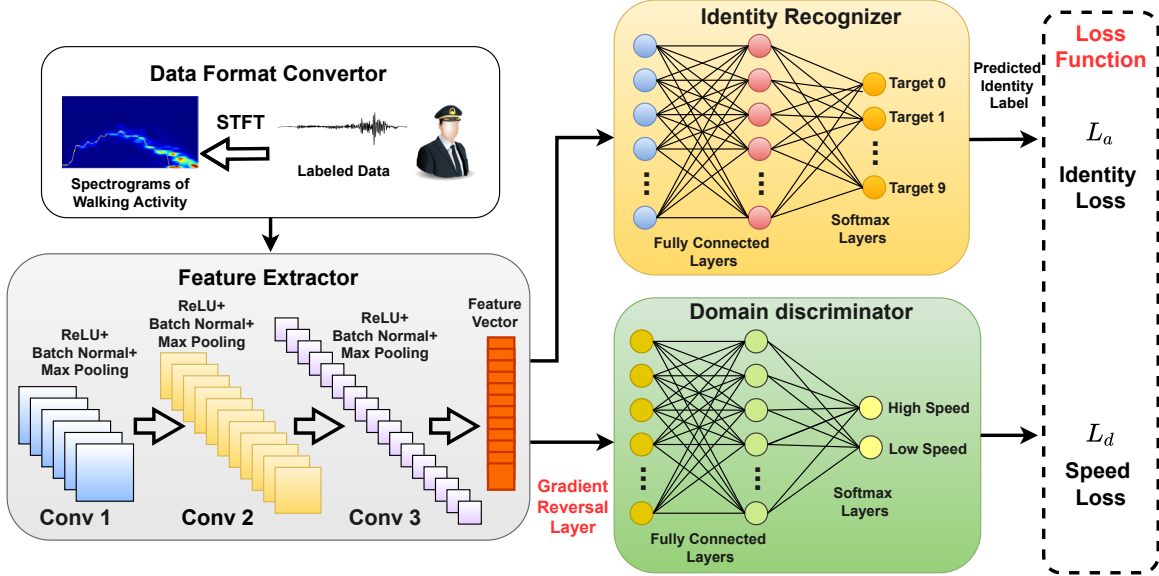


Fig. 10: Overview of domain adversarial learning based gait recognition model

### B. Feature Extractor

We employed CNNs to extract identity features, which are widely used in human identification tasks. First, the feature extractor  $G_f$  built on the CNN transforms the input time-frequency graph into a  $D$ -dimensional latent feature representation  $f \in \mathbb{R}^D$ . We assumed that all parameters of the feature extractor are  $\theta_f$ . For a given input  $X$ , we can extract the potential feature vector  $f$  as follows:

$$f = G_f(X; \theta_f), \quad (12)$$

Specifically, we use 3-layer stacked CNN to extract the features. In each layer of the CNNs, a 2D convolution kernel is first used to calculate 2D feature graphs representing the unique identities of different users. Next, the batch normal layer was used to normalize the mean and variance of the data for each layer. Finally, a rectified linear unit (ReLU) was used to introduce nonlinearity and a max-pooling layer to reduce the size of the representation.

### C. Identity Recognizer

Based on the feature representation  $f$  output by the feature extractor, the identity recognizer uses two full connection layers followed by an activation function to learn the representation  $Z_i$  of the latent space of the input data  $X$  as follows:

$$Z_i = \text{Softplus}(W_f f_i + b_f), \quad (13)$$

where  $W_f$  and  $b_f$  are the parameters to be learned and, Softplus is an activation function used to introduce nonlinearity. To predict the identity labels, we need to map the feature representation  $Z_i$  to a new latent space  $\mathbb{R}^C$ . Where  $C$  denotes the number of identity labels. In addition, an Softmax layer was used to predict user identities. Given the input feature representation  $Z_i$ , the mapping function is defined as

$$\hat{y}_i = \text{Softmax}(W_z Z_i + b_z), \quad (14)$$

where  $W_z$  and  $b_z$  are the parameters to be learned and  $\hat{y}_i$  represents the probability obtained by the model's prediction of the label to which the data belongs. We use the cross-entropy function to calculate the loss between the predicted and true values, as follows:

$$L_a = -\frac{1}{|K|} \sum_{k=1}^{|K|} \sum_{c=1}^{|C|} y_{kc} \log(\hat{y}_{kc}), \quad (15)$$

where  $|K|$  is the number of labeled data and  $y_{kc}$  is the one-hot vector of the true identity labels. In the training process, by minimizing the loss  $L_a$ , the model can learn the identity-discriminative features and obtain good identity prediction accuracy.

### D. Domain Discriminator

In our adversarial network model, the domain refers to the walking speed of the target. The reasons behind this definition are as follows: In actual scenarios, people tend to change their walking speed actively or passively, and the reasons for changing their walking speed may include weight-bearing state, health state, emotional state, etc. However, the existing wireless sensing technology is based on the Doppler effect. This means that the signal received by the receiver is very sensitive to changes in the speed of the target. When the walking speeds of the training set and the test set don't match up, the accuracy of the model's predictions falls down by a great deal.

For our domain discriminator to be able to predict the domain label of the input data, we similarly use two full connection layers followed by an activation function. The feature vector  $f \in \mathbb{R}^D$  is extracted by the feature extractor  $G_f$  to the distribution  $\mathcal{D}$  of the domain label, as follows:

$$U_i = \text{Softplus}(W_u f_i + b_u), \quad (16)$$

$$\hat{d}_i = \text{Softmax}(W_d U_i + b_d), \quad (17)$$

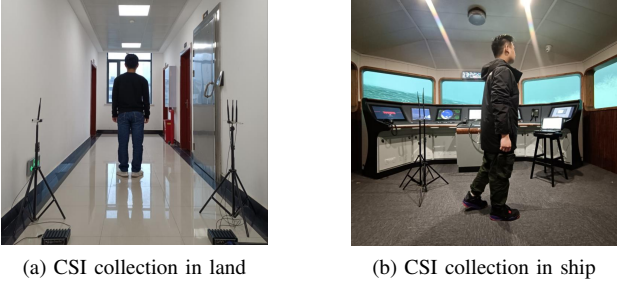


Fig. 11: Experiments scenes in land and ship.

TABLE I: Characteristics of the 10 targets

Target	T0	T1	T2	T3	T4	T5	T6	T7	T8	T9
Height(m)	1.72	1.65	1.70	1.76	1.68	1.87	1.80	1.74	1.73	1.78
Weight(kg)	62	46	68	80	57	76	78	64	61	85
Gender	M	F	M	M	F	M	M	M	M	M
Age	24	23	24	31	21	21	27	26	24	26

where  $W_u$ ,  $b_u$ ,  $W_d$ ,  $b_d$  are the parameters, and  $U_i$  is the representation of the feature vector  $f_i$  in the latent space. In order for the domain discriminator to predict the domain label of the input data, we used the cross-entropy function as the loss between the true domain label and the predicted label, as follows:

$$L_d = -\frac{1}{|K|} \sum_{k=1}^{|K|} \sum_{s=1}^{|\mathcal{D}|} d_{ks} \log (\hat{d}_{ks}), \quad (18)$$

where  $d_{ks}$  is the one-hot vector of true domain labels. Our design goal was to make the model eventually learn domain independent features; therefore, we introduced a gradient inversion layer between the feature extractor and the domain discriminator to minimize the prediction accuracy of the domain labels. In summary, the loss function of the proposed model is expressed as follows:

$$L = L_a - \lambda L_d (\lambda > 0), \quad (19)$$

where  $-\lambda$  is the gradient inversion layer, and  $\lambda$  is a hyperparameter.

## VII. EXPERIMENTS AND EVALUATION

### A. Experimental Setup and Methodology

**Devices:** We used a pair of transmitters and receivers to capture a WiFi signal that contains gait information reflected by the human body. Specifically, we used two identical mini-PCs equipped with an Intel i5 CPU, 2-GB RAM, and Intel 5300 WiFi network cards. We installed Ubuntu 12.04, and csitool [41] on the PC set the operating band to 5 GHz, channel bandwidth to 20 MHz, and the packet sending frequency to 1000 packets/s. The transmitting end uses one antenna, and the receiving end uses three antennas, resulting in  $30 \times 1 \times 3 = 90$  CSI data for each packet. After data collection, we used Python and PyTorch to prototype WiCrew on a desktop with an Nvidia GTX2080Ti GPU card, Intel I5 2.5 GHz CPU card, and 32 GB RAM.

**Data Collection:** We conducted experiments in two scenarios, namely the conventional indoor corridor and the large full-mission Navigation simulation control laboratory, as shown in

Figure 11. The Navigation Simulation and Control Laboratory, have a 6-DOF ship motion simulation platform, which can simulate the navigation state of ships under different levels of wind and waves and can be used to simulate ship vibrations of different degrees in our experiments. Our system deployment scenarios were exit passageway in key ship areas, such as bridge and engine room. Large- and medium-sized cruise ships typically have no more than ten people on duty in the cockpit and cabin, so we collected gait information from 10 volunteers and characteristics of 10 targets in Table I. Each volunteer was asked to walk along a vertical bisector of the LOS path at "fast" and "slow." Considering that normal people's comfortable walking speed is 1-1.5 m/s, we set the interval of "fast" and "slow" walking speed as 0.7-1 m/s and 1.5-1.8 m/s, respectively. We set the walking path length to 5 m, the distance between the transmitter and receiver to 1.6 m, and the antenna height as 0.85 m. Each target walked 20 times in the two environments at two speeds. Simultaneously, we conducted tests under five different vibration levels. Therefore, we finally collected  $10 \times 2 \times 2 \times 20 + 10 \times 5 \times 20 = 1800$  pieces of data.

**Baseline Method:** To evaluate the performance of our system extensively, we first implemented four state-of-the-art technologies, namely WiWho, WiFiU, WiFi-ID, and AGait. Considering that the preset path of the WiWho system was parallel to the LOS path, the relevant original settings in this study were used to evaluate its performance. The AGait system can identify the direction of the target using two WiFi links. Considering that our deployment scenario does not require identification of travel direction, we implemented AGait using only one WiFi link to achieve its identification capability. To evaluate the ability of the system to extract domain-independent features, we implemented a CNN-based gait recognition model containing only feature extractors and identifiers, which is equivalent to removing domain adaptation in WiCrew. The model design details are the same as those scheme described in Section 6 of this paper.

**Evaluation Metrics:** We defined three different evaluation metrics: *recognition accuracy* is the ratio of the preprocessed test samples to be correctly identified, which is the primary indicator of WiCrew's gait recognition ability. The *confusion matrix* indicates whether there is confusion among multiple identity classes, with each column representing the identity label predicted by the model and each row representing the actual identity label. *True positive rate* is the proportion of legitimate users in the training set that are correctly classified.

**Model Training:** Our training data set contains two labels, the identity label (from "T0" to "T9") representing the identity of 10 targets and the speed label (from "S0" to "S1") representing "fast" and "slow" walking speeds. To train the WiCrew system, both the labels must be trained simultaneously. However, because the baseline method does not require speed labels in the training process, we only used the fast walking gait data of the target for training and evaluation.

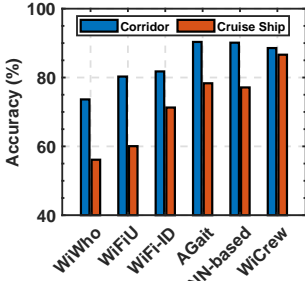


Fig. 12: Accuracy comparison

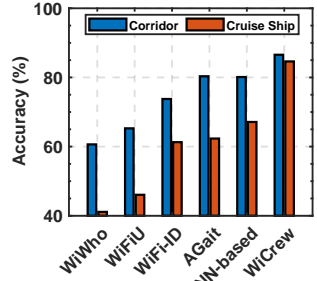


Fig. 13: Comparison in speed robustness

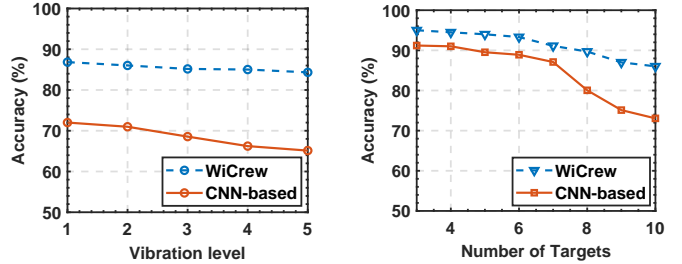


Fig. 15: Comparison in vibration robustness

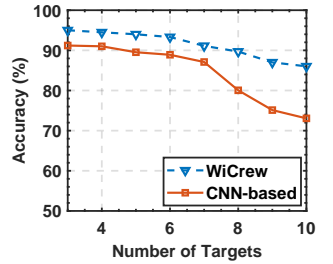


Fig. 16: Comparison in target's number robustness

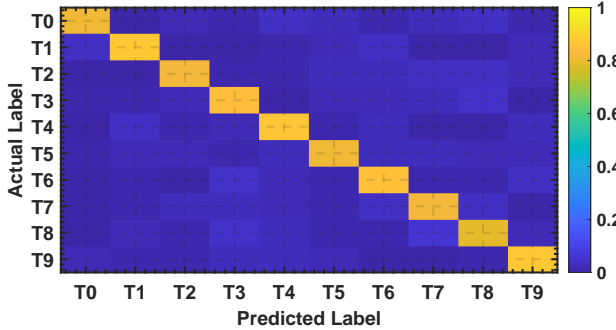


Fig. 14: The confusion matrix for recognition accuracy using WiCrew Approach

### B. Overall Performance Comparison

First, the performance of our system's gait recognition was evaluated without considering the target's speed variation. This is the same as evaluating a system only in its source domain. We utilized roughly divided training and test datasets of comparable size (speed-dependent datasets). Evaluation experiments are carried out in land and ship scenarios. Figure 12 depicts the average performance of WiCrew as well as five other baseline techniques. The results show that WiCrew's identification accuracy in the land scenarios is 88.56%, which is 14.92% higher than WiWho, 8.28% higher than WiFiU, and 6.7% higher than WiFi-ID. But it is 1.78% less than Agait and 1.56% less than CNN-based. This demonstrates that the WiCrew system's feature extractor can efficiently extract identity features from WiFi signals, which can then be used by the identity recognizer to recognize individuals. The capacity of CNN-based feature extractors to extract features is superior to that of conventional wavelet transform and signal statistical features. The severe performance degradation of WiWho in the cruise scenario may be due to a large amount of noise in the 0.2-5 Hz band. However, the addition of the domain discriminator in WiCrew removes some domain-specific identity characteristics, which is the primary reason why WiCrew's accuracy is inferior to that of Agait and CNN-based. However, when experiments were carried out on ships, the results changed. WiCrew has a recognition accuracy of 84.63%, which is more than the other five baseline approaches. This is due to the fact that WiCrew was designed specifically for the ship environment and can successfully eliminate the hull vibration component from the WiFi signal.

### C. Performance Comparison with Different Walking Speed

We also examine the robustness of gait recognition in terms of walking speed stability. We recollect the gait of volunteers walking at various speeds and utilized the original model for recognition. Figure 13 illustrates the performance of WiCrew in comparison with five other baseline approaches. Even if the target's walking speed changes, WiCrew's recognition accuracy reaches 86.56% on land and 84.63% on ships. Our system has the best accuracy in both environments, which suggests that our system selected speed-independent and identity-discriminable features. Under the same settings, WiWho and WiFiU perform significantly worse than the other four schemes. In the ship scenario, the recognition accuracy rates are 41.12% and 46.0%, and in the land scene, they are 60.64 and 65.2%, respectively. This is because WiWho and WiFiU must extract gait parameters such as gait cycle and stride length, and a change in the target's velocity will cause these two features to change dramatically, resulting in the lowest accuracy for these two systems. In Figure 14, we present the confusion matrix of the system in a speed-independent manner, i.e., the recognition accuracy of the system for the target domain sample. The results show that our system achieved an accuracy of 85% in the target domain. This indicates that the WiCrew system successfully extracted domain-independent features. As gait is loosely related to height and weight, wireless signals reflected by the body also carry bone density and fat content. Therefore, it can be seen that T0, T7, and T8 are more likely to be misjudged due to their close height and weight. Because T1 and T5 have the most significant body size differences, they have the highest recognition.

### D. Performance Comparison with Different Vibration Levels

We also examine gait recognition robustness in terms of hull vibration level to ensure that our systems can work stably on ships, even in extremely harsh environments. As we were unable to correctly measure the vibration levels of real-world ships, we conducted this experiment in the laboratory. Specifically, we used the full mission navigation simulator and the 6-DOF ship motion simulation platform to simulate the vibration degree of the ship hull when the ship encounters five different levels of wind and waves. We tested the performance of our system at five wind and wave levels and the results are shown in Figure 15. It can be seen that our system can maintain a good identification accuracy under different levels

of wind and waves. However, the identification accuracy of the baseline method decreased when the vibration level of the ship increased.

#### E. Performance Comparison With Different Number of Targets

We also examine gait recognition robustness in terms of target's number. Considering that WiCrew's gait recognition performance is related to the numbers of targets in the training set, we used the different number of targets to evaluate the WiCrew and CNN-based models. The results are shown in Figure 16. As the number of targets increased from three to ten, the average recognition accuracy of the WiCrew and CNN-based models decreased from 95.01% to 86.22% and from 91.20% to 83.06%, respectively.

### VIII. LIMITATIONS AND FUTURE WORKS

**Predefined path:** The current WiCrew system requires the crew to walk on a predefined path. The gait recognition models trained for a given walking path cannot be used for testing samples obtained on different walking paths. This is due to the fact that the phase changes of the reflected signals created by individuals traveling on distinct paths are different. This characteristic limit our system's deployment to narrow corridors, such as those access to the bridge or engine room. As part of future work, we intend to expand WiCrew to larger areas and remove this limitation.

**Multi-Person Identification:** WiCrew assumes that there is only one person walking in the WiFi area. The CFR power would contain the impacts of all users' motions when there are multiple users, making it difficult to identify each individual. As part of future work, we intend to provide WiCrew with the capacity to simultaneously recognize multiple individuals using WiFi signals with a wider bandwidth.

### IX. CONCLUSION

This paper proposed WiCrew, a WiFi-based crew gait recognition system. For the first time, WiCrew adopted EMD-ICA based signal processing method to remove the ship vibration component contained in the original CFR power. Next, using an adversarial domain adaptation model, WiCrew can remove speed-specific information from gait data while preserving identity features, thereby enabling gait recognition for target tasks at arbitrary speeds. This system can be widely deployed on ships as an access control for key areas of the ship, such as engine room, bridge, cargo hold, to ensure the safety of ship operations. We expect that our system will also be applicable to other dynamic situations, such as airplanes, subways, high-speed trains, et al. Extensive evaluation demonstrated the superiority of the proposed system.

### X. ACKNOWLEDGMENT

This work was supported by the National Natural Science Foundation of China (NSFC) under Grant No. 51979216, and the Natural Science Foundation of Hubei Province, China, under Grants No.2021CFA001 and 2022J0059.

### REFERENCES

- [1] M. Gaouette, *Cruising for trouble: Cruise ships as soft targets for pirates, terrorists, and common criminals*. ABC-CLIO, 2010.
- [2] T. R. Panko and T. L. Henthorne, "Crimes at sea: A review of crime onboard cruise ships," *IJSSTH*, no. 20, pp. 1–24, 2019.
- [3] A. Spencer and P. Tarlow, "Tourism security to tourism surety and well-being," in *Tourism Safety and Security for the Caribbean*. Emerald Publishing Limited, 2021.
- [4] R. Klein, "Sexual crimes on cruise ships: A historical perspective on security issues for passengers and crew," in *Cruise Tourism and Society*. Springer, 2012, pp. 141–151.
- [5] A. Jain, A. Ross, and S. Pankanti, "Biometrics: a tool for information security," *IEEE Transactions on Information Forensics and Security*, vol. 1, no. 2, pp. 125–143, 2006.
- [6] W. Wang, L. Yang, Q. Zhang, and T. Jiang, "Securing on-body iot devices by exploiting creeping wave propagation," *IEEE Journal on Selected Areas in Communications*, vol. 36, no. 4, pp. 696–703, 2018.
- [7] K. Peng, M. Li, H. Huang, C. Wang, S. Wan, and K.-K. R. Choo, "Security challenges and opportunities for smart contracts in internet of things: A survey," *IEEE Internet of Things Journal*, vol. 8, no. 15, pp. 12 004–12 020, 2021.
- [8] Y. Liang, S. Samtani, B. Guo, and Z. Yu, "Behavioral biometrics for continuous authentication in the internet-of-things era: An artificial intelligence perspective," *IEEE Internet of Things Journal*, vol. 7, no. 9, pp. 9128–9143, 2020.
- [9] Y. Huang, W. Wang, H. Wang, T. Jiang, and Q. Zhang, "Authenticating on-body iot devices: An adversarial learning approach," *IEEE Transactions on Wireless Communications*, vol. 19, no. 8, pp. 5234–5245, 2020.
- [10] C.-Y. Hsu, Y. Liu, Z. Kabelac, R. Hristov, D. Katabi, and C. Liu, "Extracting gait velocity and stride length from surrounding radio signals," in *Proceedings of the 2017 CHI Conference on Human Factors in Computing Systems*, ser. CHI '17. New York, NY, USA: Association for Computing Machinery, 2017, p. 2116–2126. [Online]. Available: <https://doi.org/10.1145/3025453.3025937>
- [11] C. Luo, J. Wu, J. Li, J. Wang, W. Xu, Z. Ming, B. Wei, W. Li, and A. Y. Zomaya, "Gait recognition as a service for unobtrusive user identification in smart spaces," *ACM Trans. Internet Things*, vol. 1, no. 1, mar 2020. [Online]. Available: <https://doi.org/10.1145/3375799>
- [12] Y. Chen, J. Yu, L. Kong, Y. Zhu, and F. Tang, "Rfpass: Towards environment-independent gait-based user authentication leveraging rfid," in *2022 19th Annual IEEE International Conference on Sensing, Communication, and Networking (SECON)*. IEEE, 2022, pp. 289–297.
- [13] M. Z. Ozturk, C. Wu, B. Wang, and K. R. Liu, "Gaitcube: Deep data cube learning for human recognition with millimeter-wave radio," *IEEE Internet of Things Journal*, vol. 9, no. 1, pp. 546–557, 2022.
- [14] T. Gu, Z. Fang, Z. Yang, P. Hu, and P. Mohapatra, "Mmsense: Multi-person detection and identification via mmwave sensing," in *Proceedings of the 3rd ACM Workshop on Millimeter-wave Networks and Sensing Systems*, 2019, pp. 45–50.
- [15] D. Wang, J. Yang, W. Cui, L. Xie, and S. Sun, "Caution: A robust wifi-based human authentication system via few-shot open-set gait recognition," *IEEE Internet of Things Journal*, pp. 1–1, 2022.
- [16] Y. Cao, Z. Zhou, C. Zhu, P. Duan, X. Chen, and J. Li, "A lightweight deep learning algorithm for wifi-based identity recognition," *IEEE Internet of Things Journal*, vol. 8, no. 24, pp. 17 449–17 459, 2021.
- [17] M. Chen, K. Liu, J. Ma, X. Zeng, Z. Dong, G. Tong, and C. Liu, "Moloc: Unsupervised fingerprint roaming for device-free indoor localization in a mobile ship environment," *IEEE Internet of Things Journal*, vol. 7, no. 12, pp. 11 851–11 862, 2020.
- [18] T. R. Lin, J. Pan, P. J. O'Shea, and C. K. Mechefske, "A study of vibration and vibration control of ship structures," *Marine Structures*, vol. 22, no. 4, pp. 730–743, 2009.
- [19] S.-K. Lee, M. Liao, and S. Wang, "Propeller-induced hull vibration—analytical methods," in *Proceedings of the second international ship noise and vibration conference. London, UK, June*, vol. 28. Citeseer, 2006.
- [20] Y. Zeng, P. H. Pathak, and P. Mohapatra, "Wiwho: Wifi-based person identification in smart spaces," in *2016 15th ACM/IEEE International Conference on Information Processing in Sensor Networks (IPSN)*. IEEE, 2016, pp. 1–12.
- [21] W. Wang, A. X. Liu, and M. Shahzad, "Gait recognition using wifi signals," in *Proceedings of the 2016 ACM International Joint Conference on Pervasive and Ubiquitous Computing*, 2016, pp. 363–373.

- [22] C. Kirtley, M. W. Whittle, and R. Jefferson, "Influence of walking speed on gait parameters," *Journal of biomedical engineering*, vol. 7, no. 4, pp. 282–288, 1985.
- [23] F. Sun, C. Mao, X. Fan, and Y. Li, "Accelerometer-based speed-adaptive gait authentication method for wearable iot devices," *IEEE Internet of Things Journal*, vol. 6, no. 1, pp. 820–830, 2019.
- [24] G. Rilling, P. Flandrin, P. Goncalves *et al.*, "On empirical mode decomposition and its algorithms," in *IEEE-EURASIP workshop on nonlinear signal and image processing*, vol. 3, no. 3. Citeseer, 2003, pp. 8–11.
- [25] E. Oja and Z. Yuan, "The fastica algorithm revisited: Convergence analysis," *IEEE transactions on Neural Networks*, vol. 17, no. 6, pp. 1370–1381, 2006.
- [26] L. Lee and W. E. L. Grimson, "Gait analysis for recognition and classification," in *Proceedings of Fifth IEEE International Conference on Automatic Face Gesture Recognition*. IEEE, 2002, pp. 155–162.
- [27] J. Han and B. Bhanu, "Individual recognition using gait energy image," *IEEE transactions on pattern analysis and machine intelligence*, vol. 28, no. 2, pp. 316–322, 2005.
- [28] N. Takemura, Y. Makihara, D. Muramatsu, T. Echigo, and Y. Yagi, "Multi-view large population gait dataset and its performance evaluation for cross-view gait recognition," *IPSJ Transactions on Computer Vision and Applications*, vol. 10, no. 1, pp. 1–14, 2018.
- [29] Z. Dong, Y. Lu, G. Tong, Y. Shu, S. Wang, and W. Shi, "Watchdog: Real-time vehicle tracking on geo-distributed edge nodes," *ACM Trans. Internet Things*, jul 2022, just Accepted. [Online]. Available: <https://doi.org/10.1145/3549551>
- [30] W. Cheng, R. Wen, H. Huang, W. Miao, and C. Wang, "Optdp: Towards optimal personalized trajectory differential privacy for trajectory data publishing," *Neurocomputing*, vol. 472, pp. 201–211, 2022. [Online]. Available: <https://www.sciencedirect.com/science/article/pii/S0925231221016271>
- [31] G. Yang, W. Tan, H. Jin, T. Zhao, and L. Tu, "Review wearable sensing system for gait recognition," *Cluster Computing*, vol. 22, no. 2, pp. 3021–3029, 2019.
- [32] Z. Dong, B. Lu, L. He, P. Cheng, Y. Gu, and L. Fang, "Exploring smartphone-based participatory computing to improve pervasive surveillance," ser. SenSys '13. New York, NY, USA: Association for Computing Machinery, 2013. [Online]. Available: <https://doi.org/10.1145/2517351.2517388>
- [33] T. H. M. Zaki, M. Sahrim, J. Jamaludin, S. R. Balakrishnan, L. H. Asbulah, and F. S. Hussin, "The study of drunken abnormal human gait recognition using accelerometer and gyroscope sensors in mobile application," in *2020 16th IEEE International Colloquium on Signal Processing & Its Applications (CSPA)*. IEEE, 2020, pp. 151–156.
- [34] S. U. Yunas, A. Alharthi, and K. B. Ozanyan, "Multi-modality fusion of floor and ambulatory sensors for gait classification," in *2019 IEEE 28th International Symposium on Industrial Electronics (ISIE)*. IEEE, 2019, pp. 1467–1472.
- [35] J. Zhang, B. Wei, W. Hu, and S. S. Kanhere, "Wifi-id: Human identification using wifi signal," in *2016 International Conference on Distributed Computing in Sensor Systems (DCOSS)*. IEEE, 2016, pp. 75–82.
- [36] Y. Xu, W. Yang, M. Chen, S. Chen, and L. Huang, "Attention-based gait recognition and walking direction estimation in wi-fi networks," *IEEE Transactions on Mobile Computing*, vol. 21, no. 2, pp. 465–479, 2020.
- [37] Y. ZHANG, Y. ZHENG, G. ZHANG, K. QIAN, C. QIAN, and Z. YANG, "Gaitsense: Towards ubiquitous gait-based human identification with wi-fi," *ACM Trans. Sensor Netw*, vol. 18, no. 1, pp. 1–24, 2021.
- [38] L. Deng, J. Yang, S. Yuan, H. Zou, C. X. Lu, and L. Xie, "Gaitfi: Robust device-free human identification via wifi and vision multimodal learning," *IEEE Internet of Things Journal*, pp. 1–1, 2022.
- [39] J. Zhang, Z. Chen, C. Luo, B. Wei, S. S. Kanhere, and J. Li, "Metaganfi: Cross-domain unseen individual identification using wifi signals," *Proc. ACM Interact. Mob. Wearable Ubiquitous Technol.*, vol. 6, no. 3, sep 2022. [Online]. Available: <https://doi.org/10.1145/3550306>
- [40] W. Wang, A. X. Liu, M. Shahzad, K. Ling, and S. Lu, "Understanding and modeling of wifi signal based human activity recognition," in *Proceedings of the 21st annual international conference on mobile computing and networking*, ser. MobiCom '15. Association for Computing Machinery, 2015, pp. 65–76.
- [41] D. Halperin, W. Hu, A. Sheth, and D. Wetherall, "Tool release: Gathering 802.11 n traces with channel state information," *ACM SIGCOMM Computer Communication Review*, vol. 41, no. 1, pp. 53–53, 2011.



**Kezhong Liu** received the B.S. and M.S. degrees in marine navigation from the Wuhan University of Technology(WUT), Wuhan, China, in 1998 and 2001, respectively. He received the Ph.D. degree in communication and information engineering from the Huazhong University of Science and Techonogy, Wuhan, China, in 2006. He is currently a professor with School of Navigation, WUT. His active research interests include indoor localization technology and data mining for ship navigation.



**Dashuai Pei** received the BS degree in Automation from the Northwest Minzu University, Lanzhou, China, in 2018, and the MS degree in traffic and transportation engineering, in 2022, from the Wuhan University of Technology, Wuhan, China, where he is currently working toward the Ph.D. degree. His research interests are in wireless sensing.



**Mozi Chen** received the B.S. degree in electric engineering from the Hubei University of Technology, China, in 2013. He received the M.S. and Ph.D. degree in navigation engineering from the Wuhan University of Technology (WUT), China, in 2016 and 2020. He is currently an associate researcher in WUT. His research work has been focusing on wireless sensing techniques and machine learning algorithms for human localization, emergency navigation and activity recognition in mobile environment, i.e., cruise ships.



**Shengkai Zhang** received his Ph.D. degree from the EIC Department, Huazhong University of Science and Technology (HUST) in 2021. He received his M.Sc and M.Phil degrees from HUST and Hong Kong University of Science and Technology in 2012 and 2014, respectively. He is currently an associate professor at Wuhan University of Technology (WUT). His recent research interests include state estimation, wireless sensing, mobile computing, multi-sensor fusion, robot control and planning.



**Xuming Zeng** received the Ph.D. degree in communication engineering from the China University of Geosciences, Wuhan, China, in 2018. He is currently pursuing the Ph.D. degree in traffic and transportation engineering with the School of Navigation, Wuhan University of Technology, Wuhan. He has been studying wireless ad-hoc network for shipboard environment with the Wuhan University of Technology since 2019. His research interests include routing protocols, MAC, QoS, clustering, and reliable wireless transmission.



**Kai Zheng** received the Ph.D. degree with the School of Geodesy and Geomatics, Wuhan University, in 2020. He is currently an associate researcher with the Wuhan University of Technology. His research interests are GNSS precise positioning techniques.



**Chunshen Li** received the B.S. degree in computer science from Wuhan University, Wuhan, China, in 2019, and the M.S. degree from Wuhan University of Technology, Wuhan, China, in 2022. He is currently pursuing the Ph.D. degree with the School of Electronic Information and Communications, Huazhong University of Science and Technology. His research interests include computer vision, wireless sensing, and autonomous driving.